Diffusion barrier caused by 1×1 and 7×7 on Si(111) during phase transition

H. Hibino,[1,2] C.-W. Hu,[1] T. Ogino,[2] and I. S. T. Tsong[1]
[1]*Department of Physics and Astronomy, Arizona State University, Tempe, Arizona 85287-1504*
[2]*NTT Basic Research Laboratories, NTT Corporation, Atsugi, Kanagawa 243-0198, Japan*
(Received 13 April 2001; published 16 November 2001)

Low-energy electron microscopy was used to study thermal decay of islands and vacancy islands on Si(111) at the coexistence of 1×1 and 7×7 during the phase transition. Slower surface mass diffusion on 7×7 than on 1×1, coupled with preferential formation of 7×7 on the upper terrace of a step, causes a diffusion barrier during the phase transition, resulting in an asymmetry in the thermal decay rate between island and vacancy island. The diffusion barrier also makes the mass flow induced by the atom density difference between 1×1 and 7×7 asymmetric in the step-up and step-down directions.

DOI: 10.1103/PhysRevB.64.245401 PACS number(s): 68.35.Bs, 68.35.Fx, 68.37.Nq

Much attention has been devoted recently to understand the processes involved in surface mass transport.[1–3] In order to predict how the surface morphology changes during annealing, epitaxial growth, and/or sublimation, this understanding is essential due to the increasing demand for precision in fabricating nanostructures. Crystal surfaces have various atomic structures depending on thermodynamic and/or kinetic conditions. Two different surface structures coexist on a surface under situations such as phase transition,[4] epitaxial growth,[5] and chemical reaction.[6] These different structural phases have different properties of surface mass transport. Understanding the mass transport on a surface consisting of multiple phases is of practical importance as well as scientific interest.

In this paper, we investigate mass transport on Si(111) during the 1×1 -to- 7×7 phase transition as a prototypical system with two different surface structural phases. We have already reported using low-energy electron microscopy (LEEM) that the surface mass diffusion constant on 1×1 is larger than that on 7×7.[7] Here we show that this difference in the surface mass diffusion constant, coupled with the preferential nucleation of 7×7 at the upper step edge, will lead to an asymmetric diffusion barrier during the phase transition. This barrier causes selective slowing down of the thermal decay of a vacancy island during the phase transition, whereas islands and vacancy islands decay with similar rates above or below the phase transition. Due to the higher atom density in 1×1 than 7×7,[8] excess atoms are created and diffuse to steps during the 1×1 -to- 7×7 phase transition. The asymmetric diffusion barrier also plays an important role in this step motion.

We used two kinds of Si(111) samples. One is nominally flat, and the other is patterned by the standard lithographic technique. On the nominally flat Si(111) surface, because of the mechanical stress on the sample due to clamping in our sample mount, screw dislocations were introduced into the sample during high temperature annealing. Two-dimensional islands and vacancy islands were created by the intersection of the original steps with steps newly created by the dislocation motion. Deposition of Si from a Si evaporator was also used to form islands. On the patterned substrate, we observed islands at the top of three-dimensional mounds and vacancy islands at the bottom of three-dimensional craters. The temperature was measured using an infrared pyrometer. In this paper, we define the critical temperature T_c of the 1×1 -to-7×7 phase transition as a temperature at which 7×7 begins to nucleate continuously at the step edge, and the measured temperatures were calibrated by setting $T_c = 860\,^{\circ}\mathrm{C}$.[9] Typical incident electron energy of LEEM was 10 eV. In the bright-field LEEM images at this energy, the 7×7 domains appear bright while the 1×1 domains appear dark.[10] The step-up or step-down direction was determined by the observation that 7×7 nucleates at the upper step edge.[4]

We examine the real-time thermal decay of three islands and a vacancy island, all located on the floor of a larger vacancy island, *in situ* using LEEM as illustrated in the inset in Fig. 1. The measured size evolutions with time were compared with calculations based on solving the diffusion equations under appropriate boundary conditions. We first show the diffusion equation and boundary conditions on a surface with a single phase denoted as *A*. The diffusion equation is given by Burton, Cabrera, and Frank as[11]

$$\frac{\partial c}{\partial t} = D_A \nabla^2 c - \frac{c}{\tau_A} + F, \tag{1}$$

where c is the adatom concentration, D_A and τ_A are the diffusion constant and the adatom lifetime on the *A* phase, respectively, and F is the deposition flux. The boundary conditions at the step edges are[12]

$$\pm \mathbf{n}(D_A \boldsymbol{\nabla} c)_{\pm} = K_{A\pm}(c_{\pm} - c_{\mathrm{eq}}), \tag{2}$$

where $\mathbf{n}$ is the unit normal vector at the step from the upper terrace $(-)$ to the lower terrace $(+)$, and K_{A+} and K_{A-} are the kinetic coefficients of atom incorporation at the step for the lower and upper terraces, respectively, and c_{eq} is the equilibrium adatom concentration at the step edge. In the steady state where neither sublimation nor deposition occurs, Eq. (1) is reduced to the Laplace equation. The diffusion equation was solved under the boundary conditions using the finite element method in the actual geometry determined experimentally. The atom fluxes were calculated at the edges of

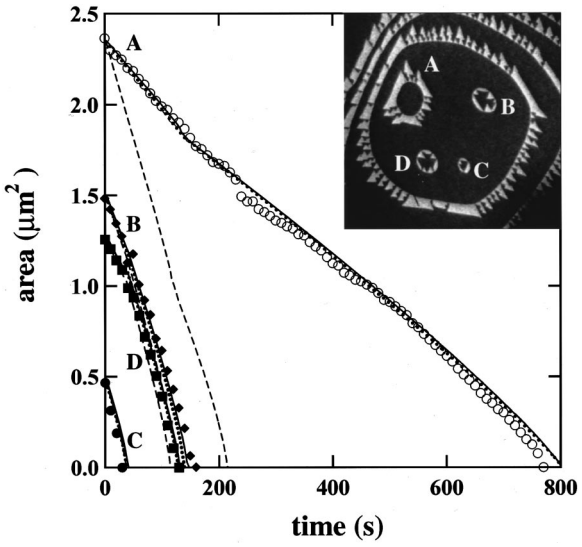

FIG. 1. Time evolution of a set of islands and vacancy island located inside a larger vacancy island at 857 °C. Inset is the bright-field LEEM image at $t=0$ s with a field of view of 12.5 μm. The incident electron energy was 10 eV. The vacancy island is indicated by *A*, and the islands are indicated by *B*, *C*, and *D*. The data points in the plots denote the measured areas. Dashed and dotted lines are results calculated by solving diffusion equation on single phase. Solid lines are calculated under the condition that the vacancy island is surrounded by 7×7 with the width of 0.2 μm. Details of the calculation procedures and the values of kinetic coefficients are given in the text. The step stiffness of 2.2×10^{-10} J m^{-1} (Ref. 15) and $Dc^0_{eq}=6.4\times10^6$ s^{-1} on 1×1 were used in these calculations.

the islands and vacancy islands from the adatom concentration, from which the island and vacancy island areas were determined a certain time later. The diffusion equation was solved again in the new geometry. The size evolution was calculated by repeating the procedures. The details of the calculation method are given in Ref. 7.

We measured the size evolutions of islands and a vacancy island at five different temperatures near T_c, and compared them with the calculations. At T_c+5 K, the surface is entirely covered with 1×1. At T_c-9 K and T_c-14 K, the surface is mostly covered with 7×7 except for narrow 1×1 regions at the lower side of the steps and at 7×7 domain boundaries. In these cases, the measured size evolutions of the islands and vacancy island were fitted reasonably by solving the single-phase diffusion equation.[7] Additionally, the calculations did not require asymmetry in the kinetic coefficient between the upper and lower terraces. Such an asymmetry is nothing more than the Ehrlich-Schwoebel (ES) barrier.[13] Therefore, we have shown that the thermal decay of micrometer-sized islands and vacancy islands on a single-phase Si(111) surface at high temperatures can be analyzed without taking the ES barrier into consideration.

However, at T_c and T_c-3 K, the vacancy island decayed at a slower rate than that expected from the calculations without the ES barrier. Figure 1 shows the size evolutions of islands and a vacancy island at T_c-3 K. First, we analyzed

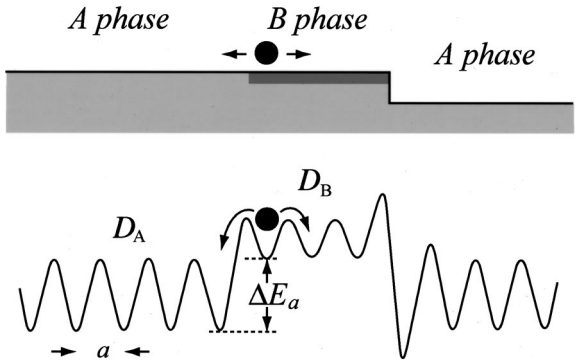

FIG. 2. Schematic potential diagram for adatom diffusion on the surface with two phases *A* and *B*.

the evolutions using Eq. (1) for the single phase. The calculated results without the ES barrier, $aK_+/D=aK_-/D=1$, indicated by the dashed lines in Fig. 1 did not reproduce the size evolutions of the islands and vacancy island, where a is the lattice constant. The best fit indicated by the dotted lines in Fig. 1 was obtained at $aK_+/D=1$ and $aK_-/D=1.6\times10^{-4}$. At T_c, we needed $aK_-/D=6.4\times10^{-4}$ to fit the experiment. These results seem to indicate that the ES barrier appears only in a narrow temperature window just below T_c. At T_c and T_c-3 K, there are 1×1 and 7×7 on the lower and upper sides of the step, and the 7×7 region is wider at T_c-3 K than at T_c. Therefore, the ES barrier may be characteristic to the step whose lower and upper sides are, respectively, 1×1 and 7×7, and the value may depend on the width of 7×7. However, the ES barrier should be mainly determined by the local atomic structure around the step, and there is a narrow 1×1 region on the lower side of the step even at T_c-9 K. It is therefore difficult to reconcile the existence of the ES barrier within such a narrow temperature window.

In this situation, we propose a model to explain the selective slowing down of the vacancy island decay without the ES barrier. This model includes two important factors. First, the surface mass diffusion constant on 1×1 is larger than that on 7×7. Secondly, the 7×7 reconstruction preferentially nucleates at the upper step edges. As the phase transition commences, the vacancy island is surrounded by 7×7 with a smaller surface mass diffusion constant but the island is still surrounded by 1×1 on the lower terrace. Because 7×7 restricts the diffusion of terrace atoms into the vacancy island, the decay of the vacancy island is thereby slowed down. We check the validity of this model by solving the diffusion equation on the surface with two phases different in the properties of mass transport.

We constructed the diffusion equations and boundary conditions on the surface with *A* and *B* phases assuming a simple potential diagram for adatom diffusion as shown in Fig. 2. The diffusion equations on *A* and *B* phases are written in the same form as Eq. (1) by using the diffusion constant and adatom lifetime on each phase. The boundary conditions at the lower and upper edges of the step are also simple extension of Eq. (2), and are written, respectively, as

$$\mathbf{n}(D_A\nabla c)_+ = K_{A+}(c - c_{\mathrm{eq}})_+ , \tag{3a}$$

$$-\mathbf{n}(D_B\nabla c)_- = K_{B-}(c - c_{\mathrm{eq}}). \tag{3b}$$

These boundary conditions at the step are not enough to solve the two diffusion equations on the *A* and *B* phases, and a boundary condition at the phase boundary is necessary. This boundary condition is written as[14]

$$\mathbf{n}(D_A\nabla c)_A = \mathbf{n}(D_B\nabla c)_B = \frac{D_B}{a}[Pc_B - c_A], \tag{4}$$

where **n** is a unit normal vector at the phase boundary from *A* to *B*. $P=\exp[\Delta E_a/k_BT]$, where ΔE_a is the difference between the adatom formation energies on *A* and *B*, k_B is the Boltzman constant, and *T* is the temperature. *P* is also expressed as $c^0_{\mathrm{eq}}(B)/c^0_{\mathrm{eq}}(A)$, where $c^0_{\mathrm{eq}}(A)$ and $c^0_{\mathrm{eq}}(B)$ are the equilibrium adatom concentration at the straight *A* and *B* steps, respectively.

In order to solve the diffusion equations on the surface with *A* and *B* phases, we need to know the difference in the diffusion constant, kinetic coefficient, and adatom formation energy (same as the equilibrium adatom concentration) between *A* and *B*. However, because mass transport on Si(111) near the phase transition temperature is governed by diffusion,[7,15] the time evolution does not depend strongly on the kinetic coefficients. Therefore, we assumed $aK_{A(B)\pm}/D_{A(B)}=1$. We also found that the calculated time evolutions do not depend separately on *D* and c^0_{eq}, but depend on their multiple Dc^0_{eq}. We have already estimated $D_{7\times7}c^0_{\mathrm{eq}}(7\times7)/D_{1\times1}c^0_{\mathrm{eq}}(1\times1)=0.05$ around T_c.[16] We used this value to simulate the evolutions of the island and vacancy island areas as shown in Fig. 1. However, the 7×7 domain around the vacancy island has a complicated shape, and the shape changed with time in a manner that was difficult to predict. Therefore, we first assumed that the vacancy island is surrounded by a continuous 7×7 domain with the width *l*. The calculations showed that the decay rate of the vacancy island strongly depends on *l*. As *l* increases, the time taken for the vacancy island to disappear rapidly increases initially but is saturated later, which explains the reason why the ES effect changes with the 7×7 width. The size evolutions calculated at $l=0.2\ \mu$m are indicated by sold lines in Fig. 1. The agreement between the experiment and calculation is quite reasonable. However, this *l* value is less than half of the actual 7×7 width surrounding the vacancy island *A* in Fig. 1. This discrepancy arises because in reality the vacancy island was not uniformly surrounded by 7×7, but with gaps of 1×1 which eventually became domain boundaries. These 1×1 gaps served as preferential diffusion paths of adatoms, which would cause a faster decay than the idealized vacancy island surrounded by a uniform 7×7 band.

The next step is to calculate the size evolution including the actual 7×7 domain shape. However, as mentioned earlier, we could not predict how the 7×7 domains change in shape with time. Therefore, we first obtained the decay rate of the vacancy island as a function of the area from sequential frame-captured LEEM video images. Then, we calculated the decay rate using the positions of the steps and 7×7 domains determined from the LEEM images. In these calculations, the steps outside the larger vacancy island were ignored. Additionally, only the 7×7 domain around the vacancy island *A* contributes to the decay rate. Figures 3(b) and 3(d) show LEEM images taken at $t=0$ and 140 s in the same experiment that contributed to the data in Fig. 1, and Figs. 3(c) and 3(e) show the corresponding geometries of the steps and 7×7 domains used in the calculations. In Fig. 3(a), the measured and calculated decay rates are plotted as a function of the vacancy island area by the open and filled circles, respectively. The solid and dashed

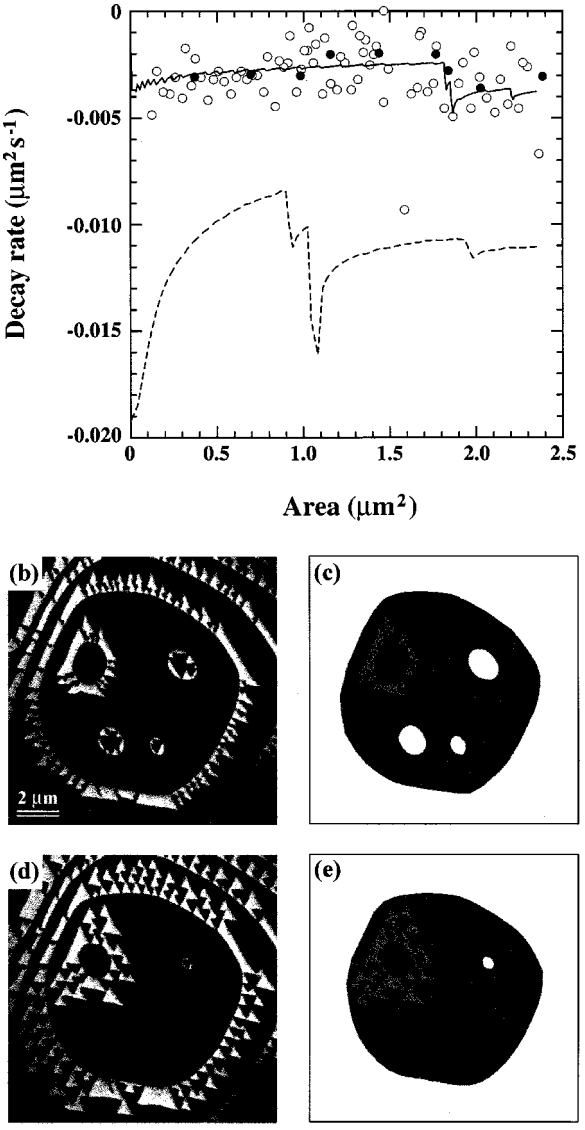

FIG. 3. The dependence of the decay rate on the area, which was converted from the time evolution of the vacancy island area shown in Fig. 1. Open circles denote the measured data. Solid and dotted curves are converted from the calculated results indicated by solid and dotted plots in Fig. 1. (b) and (d) are LEEM images taken at $t=0$ s and $t=140$ s with a field of view of 12.5 μm. (c) and (e) are corresponding geometries of the steps and 7×7 domains used for calculating the decay rate. The calculated decay rates are indicated by filled circles in (a).

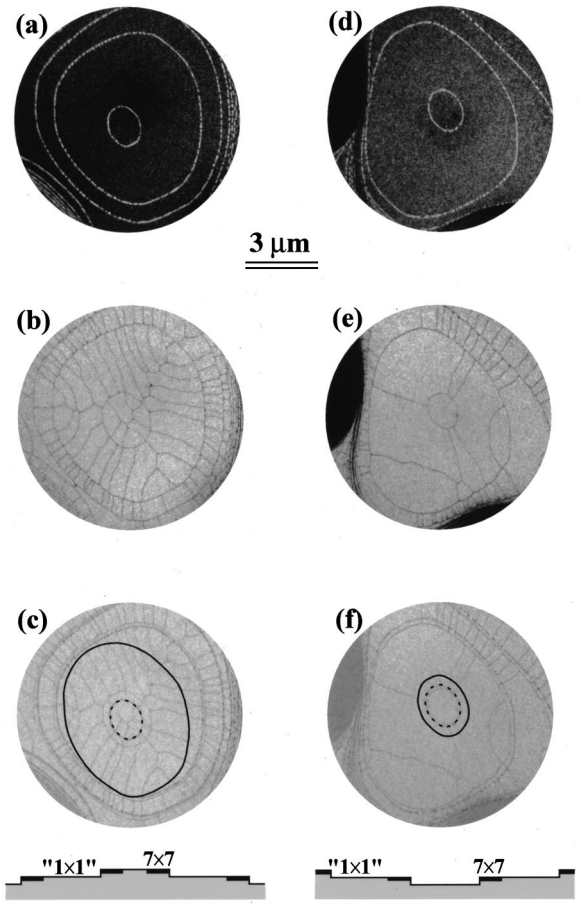

FIG. 4. (a)–(c) LEEM images of an island on a larger island. (d)–(f) a vacancy island inside a larger vacancy island. (a) and (d) were taken before the 1×1-to-7×7 phase transition. (b) and (e) after the phase transition. In (c), (a) is overlaid on (b) after the contrast of (a) was reversed, and (f) was made from (d) and (e) by the same procedure. The dotted lines in (c) and (f) indicate the positions of the island and vacancy island edges before the phase trasnsition, respectively, and the solid lines indicate the adatom capture areas of the center island and center vacancy island, which were calculated assuming the difference in the atom density between 1×1 and 7×7 is 0.065 bilayers.

curves in Fig. 3(a) were obtained by converting the data corresponding to the solid and dashed plots in Fig. 1 to the dependence of the decay rate on the area. Figure 3 shows that the calculated decay rates using the actual 7×7 domain shape are in reasonable agreement with the measured ones. From the above discussion, we infer that the smaller mass diffusion constant on 7×7 than on 1×1 and preferential formation of 7×7 at the upper step edges effectively causes an asymmetric diffusion barrier during phase transition, resulting in the preferential slowing down of the vacancy island decay.

The atom density in the 1×1 phase is 0.06–0.07 bilayers higher than that in the 7×7 phase.[8] Therefore, the area of the island increases and the area of the vacancy island decreases during the phase transition from 1×1 to 7×7, because excess atoms diffuse to steps. The asymmetric diffusion barrier also plays an important role in this step motion during the phase transition. Figures 4(a) and 4(b) show LEEM images of an island on a larger island before and after the phase transition. In Fig. 4(c), 4(a) is overlaid on 4(b) after the contrast of 4(a) was reversed, and the dotted line indicates the position of the center island edge before the phase transition. Figure 4(c) clearly shows that the island area increased after the phase transition. The solid line in Fig. 4(c) is the region inside which atoms created during the phase transition diffused to the top island, and was calculated assuming the difference in the atom density between 1×1 and 7×7 is 0.065 bilayers. The calculated capture area is close to the area of the larger island. This is because the asymmetric diffusion barrier appeared at the upper side of the larger island. On the other hand, in the case of a vacancy island inside a larger vacancy island [Figs. 4(d)–4(f)], the asymmetric diffusion barrier around the smaller vacancy island restricts atoms from diffusing into the smaller vacancy island. Therefore, the capture area is much smaller than the area of the larger vacancy island as shown in Fig. 4(f).

All the above discussion suggests that the asymmetric diffusion barrier caused by 1×1 and 7×7 is sufficient to explain the phenomena and the real ES barrier is unnecessary. In order to support this inference, we measured the area change of an island on a larger island during the 1×1-to-7×7 phase transition under two different conditions. Under the first condition, the islands were cooled so slowly that 7×7 nucleates only at the upper step edges. In this case, due to the asymmetric diffusion barrier, excess atoms created on the larger island prefer to diffuse to the step of the smaller island rather than to the step of the larger island. Under the second condition, the sample is cooled so quickly through the phase transition that 7×7 nucleates on the terraces as well as at the steps. In this case, the asymmetric diffusion is less pronounced. On the contrary, if there is a real ES barrier at the step, the island area should change similarly regardless of the cooling rate. We compared the capture areas of the islands cooled slowly and quickly. The capture areas were always larger on the slowly cooled sample than on the quickly cooled sample. This provides further support that the asymmetric diffusion barrier rather than the real ES barrier is the cause of the asymmetry in the thermal decay and area change between vacancy island and island during the phase transition.

In conclusion, we observed thermal decay of islands and vacancy islands on Si(111) *in situ* using LEEM. By comparing the measured size evolutions of islands and vacancy islands with calculations, we showed that the smaller surface mass diffusion constant on 7×7 compared to that on 1×1 and the preferential formation of 7×7 at the upper step edges produces the asymmetric diffusion barrier during the phase transition. This asymmetric diffusion barrier plays important roles in the surface morphology changes including the step wandering instability during Si homoepitaxial growth.[17]

We would like to thank Professor Makio Uwaha for his helpful discussion. This work was supported in part by NFS Grant No. DMR-9632635 and DMR-9986271.

[1] S. Tanaka, N. C. Bartelt, C. C. Umbach, R. M. Tromp, and J. M. Blakely, Phys. Rev. Lett. **78**, 3342 (1997).
[2] J. B. Hannon, C. Klünker, M. Giesen, H. Ibach, N. C. Bartelt, and J. C. Hamilton, Phys. Rev. Lett. **79**, 2506 (1997).
[3] K. Morgenstern, G. Rosenfeld, E. Lægsgaard, F. Besenbacher, and G. Comsa, Phys. Rev. Lett. **80**, 556 (1998).
[4] N. Osakabe, Y. Tanishiro, K. Yagi, and G. Honjo, Surf. Sci. **109**, 353 (1981).
[5] U. Köhler, J. E. Demuth, and R. J. Hamers, J. Vac. Sci. Technol. A **7**, 2860 (1989).
[6] H. H. Rotermund, W. Engel, M. Kordesch, and G. Ertl, Nature (London) **343**, 355 (1990).
[7] H. Hibino, C.-W. Hu, T. Ogino, and I. S. T. Tsong, Phys. Rev. B **63**, 245402 (2001).
[8] Y.-N. Yang and E. D. Williams, Phys. Rev. Lett. **72**, 1862 (1994).
[9] Y. Homma and N. Aizawa, Phys. Rev. B **62**, 8323 (2000).
[10] W. Telieps and E. Bauer, Surf. Sci. **162**, 163 (1985).
[11] W. K. Burton, N. Cabrera, and F. C. Frank, Philos. Trans. R. Soc. London **243**, 299 (1951).
[12] G. S. Bales and A. Zangwill, Phys. Rev. B **41**, 5500 (1990).
[13] R. L. Schwoebel and E. J. Shipsey, J. Appl. Phys. **37**, 3682 (1966).
[14] M. Uwaha (private communication).
[15] T. Ihle, C. Misbah, and O. Pierre-Louis, Phys. Rev. B **58**, 2289 (1998).
[16] In Fig. 1, because there is no 7×7 between the islands, atoms escaping from the islands diffuse mostly on the 1×1. In fact, the decay curves of islands *B-D* calculated with and without the ES barrier are almost the same. This means that we determined the value of $D_{1\times1}c^0_{eq}(1\times1)$ at 857 °C by comparing the time evolution in Fig. 1 with the calculations. In Fig. 6 of Ref. 7, the data indicated by the filled diamonds were determined similarly by comparing the experimental time evolution with the calculations. So the filled diamonds at 865, 860, and 857 °C denote the values of $D_{1\times1}c^0_{eq}(1\times1)$. That figure shows that these values change more steeply than the data above T_c. Dc^0_{eq} changes steeply between 860 and 851 °C. The data at 851 °C should be the value of $D_{7\times7}c^0_{eq}(7\times7)$. Assuming that $D_{1\times1}c^0_{eq}(1\times1)$ has an Arrhenius form, $D_{1\times1}c^0_{eq}(1\times1)$ at 851 °C is estimated to be one-half of the value at 860 °C. This decrease is not consistent with the difference in Dc^0_{eq} between 860 and 851 °C, and the difference between $D_{1\times1}c^0_{eq}(1\times1)$ and $D_{7\times7}c^0_{eq}(7\times7)$ explains the inconsistency. Thus, we obtained $D_{7\times7}c^0_{eq}(7\times7)/D_{1\times1}c^0_{eq}(1\times1)=0.05$.
[17] H. Hibino, Y. Homma, C.-W. Hu, M. Uwaha, T. Ogino, and I. S. T. Tsong (unpublished).